Trajectories of fluid particles in a periodic water-wave

Hisashi Okamoto[*] and Mayumi Shōji[†]

Abstract

We compute trajectories of fluid particles in a water-wave which propagates with a constant shape in a constant speed. The Stokes drift, which asserts that fluid particles are pushed forward by a wave, is proved in a new method. Numerical examples with various gravity and surface tension coefficients are presented.

1 Introduction

We consider two-dimensional progressive water-waves, which propagate with a constant shape in a constant speed. Fluid motion is assumed to be irrotational. We are interested in the study of trajectories of fluid particles in the stationary coordinate system. Trajectories in a coordinate system attached to the wave are easily computed by drawing contours (level curves) of the stream function. Examples are abundant, see, e.g., [22]. On the other hand, we need some care to compute trajectories in the stationary coordinate system. [20] gives some examples for gravity waves, but we do not know examples of capillary-gravity waves. The first objective of the present paper is to give some new examples. We draw trajectories of gravity, capillary-gravity, and pure capillary waves.

It is well-known (see [19] or [21]) that fluid particles in a linearized water waves of small amplitude move on a circle or an ellipse, depending on whether the depth of water is infinite or finite, respectively. Therefore, the fluid particle does not move on average, while the wave itself propagates with a non-zero speed. This is, however, a proposition which is valid only approximately. In fact, Stokes [25] discovered that a particle trajectory is not closed.

Recently A. Constantin mathematically proved in [4] that none of the trajectories in the gravity waves are closed. It is also proved even that trajectories in some linearized water-waves are not closed, either. See [7] and [8] for the case of finite and infinite depth, respectively. The second objective of the present paper is to prove non-closedness of trajectories by a method different from those in [4, 7]. Our proof may be of some use because of its simplicity.

The present paper is organized as follows. In section 2 we give an account for the background of the present problem. Following this, we prepare some notations and a mathematical framework in section 3. In section 4, we study Crapper's pure capillary waves. Gravity and capillary-gravity waves are computed in section 5. Constantin's theorem is proved in section 6. Finally in section 7, concluding remarks are presented.

[*]Research Institute for Mathematical Sciences, Kyoto University, Kyoto, 606-8502 Japan. Partially supported by JSPS Grant 20244006

[†]Department of Mathematical and Physical Sciences, Japan Women's University, 2-8-1 Mejirodai Bunkyo-ku Tokyo, 112-8681 Japan

2   Background

For historical materials on water waves, we recommend Craik [11]. Here we summarize what is necessary in the present paper.

Fluid particles in a linearized gravity waves of small amplitude move on a circle or an ellipse. This was first recognized by Green (see [15], page 280). Stokes [25] then considered higher order approximation. In the second order approximation, he found a term which is proportional to time variable, hence the particle trajectory does not close, but the fluid particle moves, on average, in the same direction as the wave. This phenomenon is now called the Stokes drift. If the reader look at photos in page 110 of [28] carefully, then he/she will find some trajectories which are not closed.

Longuett-Higgins [20] considered gravity waves of any amplitude and computed approximately the trajectories of particles. The paper also presents some laboratory experiments, which seems to agree with his theory.

From the viewpoint of modern mathematicians, Stokes's argument is not a rigorous proof of non-closedness of particle trajectories. It is Constantin [4] that first presented a rigorous proof of the Stokes drift. His result has many variants [5, 7, 8, 9, 16], which we will comment in the following sections of the present paper.

Recently the paper [1] came upon our attention. The authors of this paper computed approximate solutions of fifth order and compared them with their laboratory experiments. The agreement seem to be very good. See also [27].

These studies are concerned with irrotational waves. Particles in rotational waves behave quite differently. In fact, all the trajectories in Gerstner's wave (discovered by [14] and later independently by [23]) are circles, no matter how large the wave amplitude may be, see [19, 21, 2, 17].

3   Preliminaries

In what follows, we restrict ourselves to particles in irrotational waves. In the moving frame, where the wave profile looks stationary, we take (x, y) as the coordinates. We set $z = x + \mathrm{i}y$ and identify the complex plane with the (x, y)-plane. In the stationary coordinate system, we take (X, Y). They are related as $X = x + \gamma t, Y = y$, where γ is the propagating speed of the wave profile. Since we do not lose generality by normalizing $\gamma = -1$ and setting the wave length as 2π, we do so henceforth. Accordingly, we have $X + t + \mathrm{i}Y = x + \mathrm{i}y$. Hereafter we use the notation of [22]. The reason that we use $\gamma = -1$ rather than $\gamma = 1$ is that we need many formulas in [22], where $\gamma = -1$ was employed, and we prefer compatibility with [22] to that with [1]–[9]. [1]–[9] employs $\gamma = 1$.

The fluid is assumed to be incompressible and inviscid. The motion of fluid is assumed to be irrotational. Throughout this paper, except in subsection 6.1, we consider only progressive waves on water of infinite depth. Using the complex potential $f = U + \mathrm{i}V$, where U is the velocity potential and V is the stream function, we define ζ as

$$\zeta = \exp(-\mathrm{i}f). \qquad (1)$$

Our normalization implies that U and V are so normalized that $|U| \leq \pi, -\infty < V \leq 0$. Accordingly, ζ runs in and on the unit disk of the complex plane. Namely, $|\zeta| \leq 1$. We

define $z = x + \mathrm{i}y$ which is conformally in one-to-one correspondence with ζ and f. For later use, we define ρ and σ by $\zeta = \rho e^{\mathrm{i}\sigma}$. We now set

$$\mathrm{i}\log\frac{\mathrm{d}f}{\mathrm{d}z} = \omega = \theta + \mathrm{i}\tau, \tag{2}$$

which is regarded as an analytic function of ζ. Here ω is defined by the equality on the left hand side. The equality on the right hand side implies just that the real and imaginary parts of ω is denoted by θ and τ, respectively. ω satisfies that $\omega(0) = 0$, which simply implies that the velocity tends to unity as $\zeta \to 0$, i.e., as $y \to -\infty$.

It is shown in [22] that two-dimensional progressive waves are characterized by the following Levi-Civita equation:

$$e^{2\tau}\frac{\mathrm{d}\tau}{\mathrm{d}\sigma} - pe^{-\tau}\sin\theta + q\frac{\mathrm{d}}{\mathrm{d}\sigma}\left(e^{\tau}\frac{\mathrm{d}\theta}{\mathrm{d}\sigma}\right) = 0 \qquad (0 \leq \sigma \leq 2\pi). \tag{3}$$

Note that θ and τ in (2) are regarded as a function of ζ defined in the unit disk of the complex plane. θ and τ in (3) denote $\theta(1,\sigma)$ and $\tau(1,\sigma)$, respectively. Since an analytic function is uniquely determined by its boundary values, $\theta(\rho,\sigma)$ and $\tau(\rho,\sigma)$ are uniquely determined once $\theta(1,\sigma)$ and $\tau(1,\sigma)$ are given. Since τ is an imaginary part of the analytic function $\theta + \mathrm{i}\tau$, τ can be written as the Hilbert transform of θ. Accordingly, we have

$$\tau(\sigma) = \frac{1}{2\pi}\int_{-\pi}^{\pi}\theta(s)\cot\frac{\sigma - s}{2}\,\mathrm{d}s,$$

where $\tau(\sigma) = \tau(1,\sigma)$ and $\theta(\sigma) = \theta(1,\sigma)$. p and q in (3) are parameters:

$$p = \frac{gL}{2\pi\gamma^2}, \qquad q = \frac{2\pi T}{m\gamma^2 L}.$$

Here L is the wave length and γ is the propagation speed, g is the gravity acceleration, T is the surface tension, and m is the density of the fluid. Since we have normalized with $\gamma = -1$ and $L = 2\pi$, p is nothing but the gravity acceleration.

The issue of existence of the solutions is discussed in [26, 22].

4   Crapper's waves

Crapper's pure capillary wave, discovered by [12], is an exact solution when gravity is neglected $(p = 0)$ and the surface tension is the only force acting on the fluid surface. It is given as

$$\frac{\mathrm{d}f}{\mathrm{d}z} = \left(\frac{1 + A\zeta}{1 - A\zeta}\right)^2 \qquad (\zeta \in \mathbb{C},\ |\zeta| \leq 1), \tag{4}$$

where $-1 < A < 1$ is a real parameter, which is related to q in the following way:

$$q = \frac{1 + A^2}{1 - A^2}.$$

See [22]. Since (1) gives us

$$\frac{\mathrm{d}\zeta}{\mathrm{d}f} = -\mathrm{i}\zeta, \tag{5}$$

3

(4) implies that

$$\frac{\mathrm{d}z}{\mathrm{d}\zeta} = \frac{\mathrm{i}}{\zeta}\left(\frac{1 - A\zeta}{1 + A\zeta}\right)^2 = \mathrm{i}\left(\frac{1}{\zeta} - \frac{4A}{(1 + A\zeta)^2}\right). \tag{6}$$

Integrating this, we obtain

$$z = \mathrm{i}\left(\log\zeta + \frac{4}{1 + A\zeta} - 4\right). \tag{7}$$

Here the integral constant is chosen so that the free surface of the trivial solution (the one with $A = 0$) becomes the line segment $y = 0, -\pi \le x < \pi$. The free surface in the moving frame is obtained if we set $\zeta = e^{\mathrm{i}\sigma}$ in (7). If $0 < \rho < 1$ is fixed and σ runs in $0 \le \sigma < 2\pi$, then a particle trajectory below the free surface in the moving frame is obtained. We draw in Figure 1 some wave profiles ($\rho = |\zeta| = 1$) and particle trajectories in the water ($0 < \rho < 1$). If $|A| > 0.45467\cdots$, the wave profile has self-intersection points, and it is an unphysical solution. We must therefore consider only those solutions with $|A| < 0.45467\cdots$. See [22].

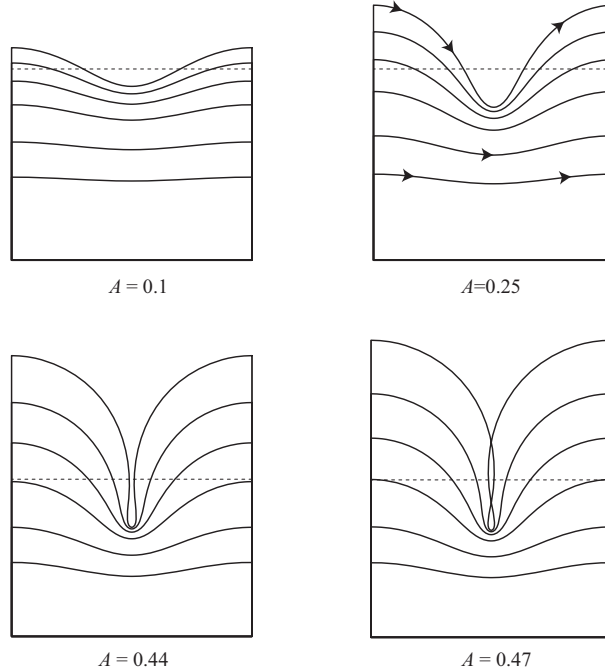

$A = 0.1$ $A=0.25$

$A = 0.44$ $A = 0.47$

Figure 1: Crapper's waves in the moving coordinates. $A = 0.1, 0.25, 0.44, 0.47$. $\rho = 0.1, 0.2, 0.4, 0.6, 0.8, 1$. The broken line shows the level $y = 0$. The arrows indicate the directions of the particles. They move from left to right.

Once the trajectory $z = z(t)$ in the moving frame is given, we can obtain the corresponding $\zeta = \zeta(t)$ by applying the inverse mapping of (7). But the concrete expression of the inverse mapping does not seem to be available, and we proceed as follows. By (6) we have

$$\frac{\mathrm{d}z}{\mathrm{d}t} = \frac{\mathrm{i}}{\zeta}\left(\frac{1 - A\zeta}{1 + A\zeta}\right)^2\frac{\mathrm{d}\zeta}{\mathrm{d}t} \tag{8}$$

On the other hand, we can obtain the complex velocity by (4). The velocity in the complex

number notation is:

$$\left(\frac{1 + A\overline{\zeta}}{1 - A\overline{\zeta}}\right)^2,$$

where the bar denotes the complex conjugate. This must be equal to $\frac{\mathrm{d}z}{\mathrm{d}t}$. Hence,

$$\left(\frac{1 + A\overline{\zeta}}{1 - A\overline{\zeta}}\right)^2 = \frac{\mathrm{i}(1 - A\zeta)^2}{\zeta(1 + A\zeta)^2}\frac{\mathrm{d}\zeta}{\mathrm{d}t}.$$

We therefore obtain

$$\frac{\mathrm{d}\zeta}{\mathrm{d}t} = \frac{\zeta|1 + A\zeta|^4}{\mathrm{i}|1 - A\zeta|^4}. \tag{9}$$

If we represent $\zeta(t)$ in the polar coordinate as $\zeta(t) = \rho(t)e^{\mathrm{i}\sigma(t)}$, (9) becomes

$$\frac{\mathrm{d}\sigma}{\mathrm{d}t} = -\left(\frac{1 + 2A\rho\cos\sigma + A^2\rho^2}{1 - 2A\rho\cos\sigma + A^2\rho^2}\right)^2 \quad \text{and} \quad \frac{\mathrm{d}\rho}{\mathrm{d}t} = 0. \tag{10}$$

We can solve this as

$$-t = \frac{-4b}{1 - b^2}\frac{\sin\sigma}{1 + b\cos\sigma} + \frac{8b^2}{(1 - b^2)^{3/2}}\tan^{-1}\left(\sqrt{\frac{1 - b}{1 + b}}\tan\left(\frac{\sigma}{2}\right)\right) + \sigma \quad (-\pi < \sigma < \pi), \tag{11}$$

where b is a parameter defined by

$$b = \frac{2A\rho}{1 + A^2\rho^2}.$$

(Since ρ is independent of t and is a constant for a given particle, we regard it as a parameter.) We have chosen the integral constant so that $t = 0$ corresponds to $\sigma = 0$. Or, instead, we may choose $\sigma' = \pi - \sigma$ to have

$$t = \frac{4b}{1 - b^2}\frac{\sin\sigma'}{1 - b\cos\sigma'} + \frac{8b^2}{(1 - b^2)^{3/2}}\tan^{-1}\left(\sqrt{\frac{1 + b}{1 - b}}\tan\left(\frac{\sigma'}{2}\right)\right) + \sigma' \quad (0 < \sigma' < 2\pi). \tag{12}$$

Here the integral constant is adjusted so that $t = 0$ at $\sigma' = 0$. When we derive (12), we should note an identity $\tan^{-1}x + \tan^{-1}\frac{1}{x} = \frac{\pi}{2}$. It is easily seen that we can choose a branch of $\tan^{-1}$ so that the right hand side of (12) becomes smooth at $\sigma' = \pi$.

We are now ready to draw trajectories in the stationary frame. By (7) and $X + \mathrm{i}Y = x - t + \mathrm{i}y$, we have

$$X = \frac{8b^2}{(1 - b^2)^{3/2}}\tan^{-1}\left(\sqrt{\frac{1 - b}{1 + b}}\tan\left(\frac{\sigma}{2}\right)\right) - \frac{1 + b^2}{1 - b^2}\frac{2b\sin\sigma}{1 + b\cos\sigma}, \tag{13}$$

$$Y = \frac{2\sqrt{1 - b^2}}{1 + b\cos\sigma} - 2 + \log\rho. \tag{14}$$

or

$$X = -\frac{8b^2}{(1 - b^2)^{3/2}}\tan^{-1}\left(\sqrt{\frac{1 + b}{1 - b}}\tan\left(\frac{\sigma'}{2}\right)\right) - \frac{1 + b^2}{1 - b^2}\frac{2b\sin\sigma'}{1 - b\cos\sigma'}, \tag{15}$$
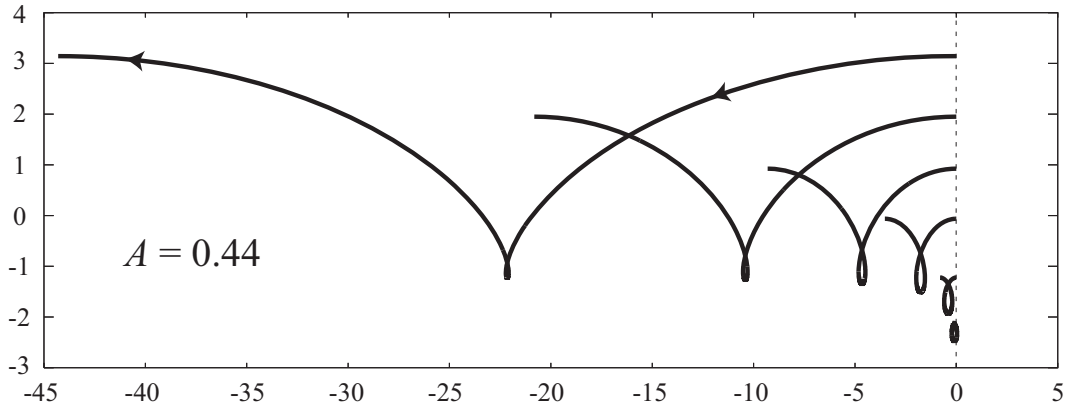
5

Figure 2: Particle trajectories in the stationary coordinates in $0 \leq \sigma' \leq 2\pi$. $A = 0.44$. $\rho = 0.1, 0.2, 0.4, 0.6, 0.8, 1$. Particles move from the right to the left.
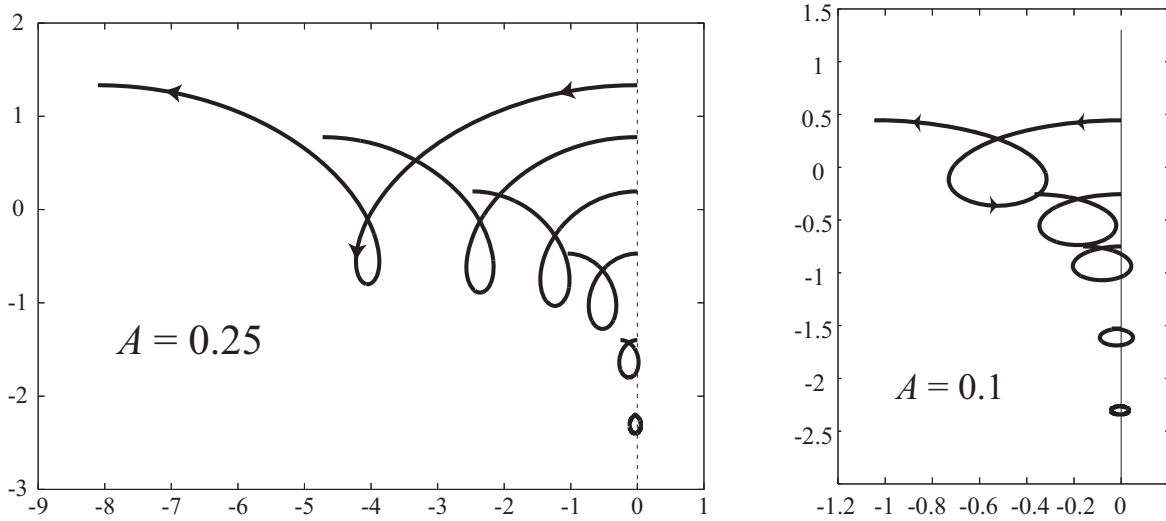

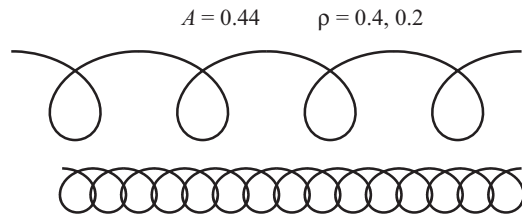Figure 3: The same as in Figure 2, but $A = 0.25$(left). $A = 0.1$(right).

Figure 4: Particle trajectories $A = 0.44$.

Either will do, but we mostly use (15) and (14) in what follows.

We now compute some trajectories. We suppose that one of the crests of the wave starts from y-axis at $t = 0$. We then consider the motion of several particles which lie on the y-axis at $t = 0$. We computed trajectories for $0 \leq \sigma' \leq 2\pi$. This implies that we draw trajectories until the particle comes to the same height as the initial position. Figure 2 shows the trajectories in the case of $A = 0.44$. We see that the particle on the free surface takes a long journey. Figure 3 shows some trajectories when $A = 0.25$ and $A = 0.1$. No trajectory in these figures is closed, and the particles are drifted leftward. Since the wave is periodic, the trajectories actually look like Figure 4.

When $A = 0.44$, we plotted in Figure 5 a trajectory which lies somewhat deep, $\rho = 0.02$. It is not closed, but is very much like a circular curve. Note that decreasing ρ implies increasing the depth and reducing the nonlinear effect. Therefore Figure 5 complies with the linear theory.
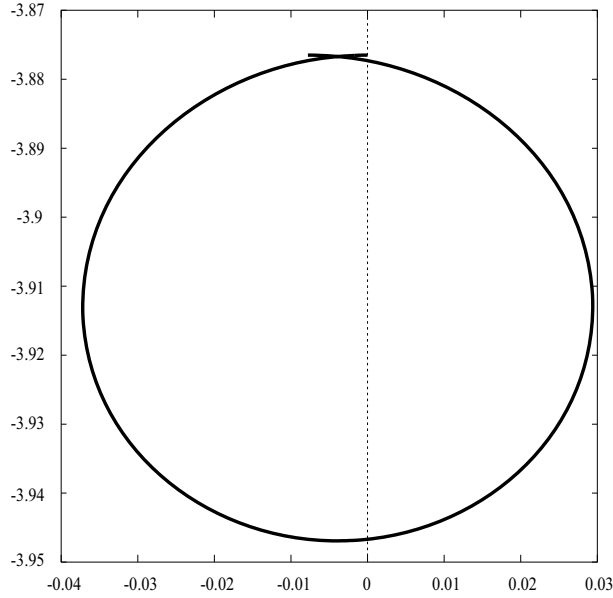

Figure 5: The particle trajectory in $0 \leq \sigma' \leq 2\pi$. $A = 0.44, \rho = 0.02$.

We now define the drift distance as

$$D(\rho) = X(\sigma' = 2\pi) - X(\sigma' = 0).$$

This is the distance between two consecutive crests in the stationary frame. As is seen from (15), it is expressed as

$$D(\rho) = -\frac{8\pi b^2}{(1 - b^2)^{3/2}} = -32\pi A^2 \rho^2 \frac{1 + A^2 \rho^2}{(1 - A^2 \rho^2)^3}. \tag{16}$$

Note that $Y(\sigma' = 0) = Y(\sigma' = 2\pi)$, whence the trajectory is closed if and only if $D(\rho) = 0$. Actually $D(\rho) < 0$ for all $\rho \in (0, 1]$, which implies that the fluid particle is drifted toward left—the same direction as the wave. A parameter defined by

$$\overline{y} = \frac{1}{2\pi} \int_{-\pi}^{\pi} y(\sigma) \, d\sigma = \log \rho$$

7

may be more intuitive than ρ, and let us employ this as the parameter representing the depth. By this, we can regard $D = D(\overline{y})$ as defined in $\overline{y} \in (-\infty, 0]$. Its graph is drawn in Figure 6. Since $D(\overline{y})$ decreases exponentially as $\overline{y} \to -\infty$, the drift is very small in deep water.
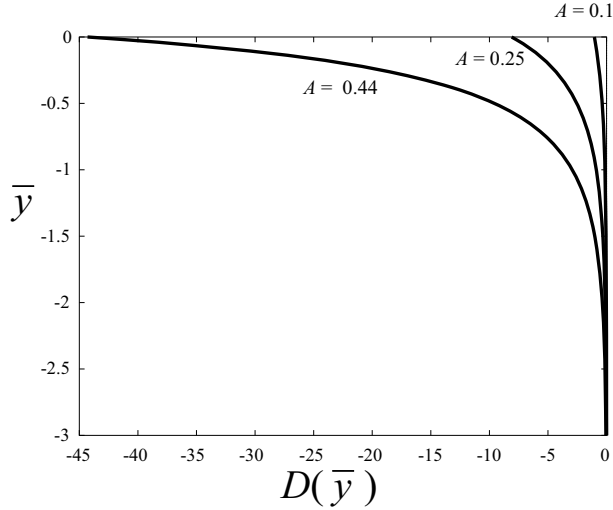

Figure 6: The drift distances for $A = 0.1, 0.25, 0.44$.

We next verify that the trajectories are almost circular in deep water. We expand (15) and (14) in small b to have

$$X = -2b \sin \sigma' - 4b^2 \sigma' - b^2 \sin 2\sigma' + O(b^3), \qquad Y = 2b \cos \sigma' + 2b^2 \cos^2 \sigma' + \log \rho - b^2 + O(b^3) \tag{17}$$

If we take only $O(b)$ terms, we have a circle. The term $-4b^2 \sigma'$ is responsible for the Stokes drift.

So far we have considered trajectories from a crest to the next crest. But the time which elapsed during this motion is different from a trajectory to a trajectory. For instance, the particle on the free surface in Figure 2 travels long distance and takes a lot of time. The travel time is considerably larger than 2π. On the other hand, the particle lying in deep water comes to the next crest in time which is close to 2π. Therefore it would be interesting to consider trajectories for a fixed time interval, say, $0 \le t \le 2\pi$. Figure 7(left) shows those parts of trajectories for $0 \le t \le 2\pi$. Figure 7(right) shows positions of particles at $t = 2\pi k/10$ ($k = 0, 1, \cdots, 10$), which started the y-axis at $t = 0$. Figure 8 shows the same data for a different A.

5   Gravity and capillary-gravity waves

We now study trajectories in the case of general (p, q). We consider only symmetric waves. Accordingly, θ is assumed to be odd in $\sigma \in (-\pi, \pi)$. We start with (3). By the Fourier-spectral method, we obtain its approximate solution

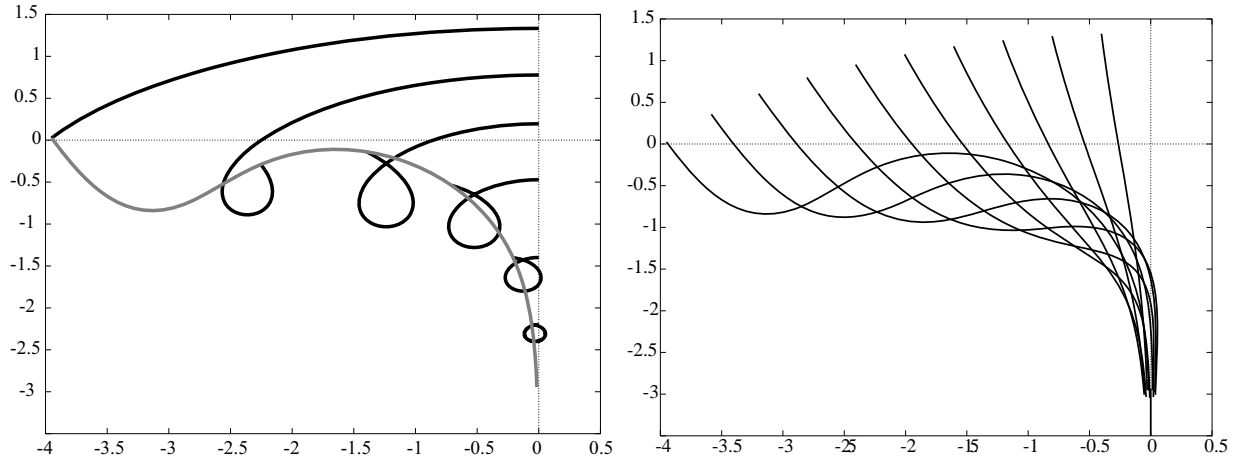$$\theta(1, \sigma) = \sum_{n=1}^{N} a_n \sin n\sigma. \tag{18}$$

8

Figure 7: Particle trajectories in $0 \leq t \leq 2\pi$. $A = 0.25, \rho = 1, 0.8, 0.6, 0, 4, 0.2, 0.1$ and $(X|_{t=2\pi}, Y|_{t=2\pi})$ with various ρ are plotted together. The Y-axis is mapped, at $t = 2\pi$, onto the gray line. (left). (X, Y) with $t = 2\pi k/10 (k = 1, 2, \cdots, 10)$ with $0.05 \leq \rho \leq 1$ (right).
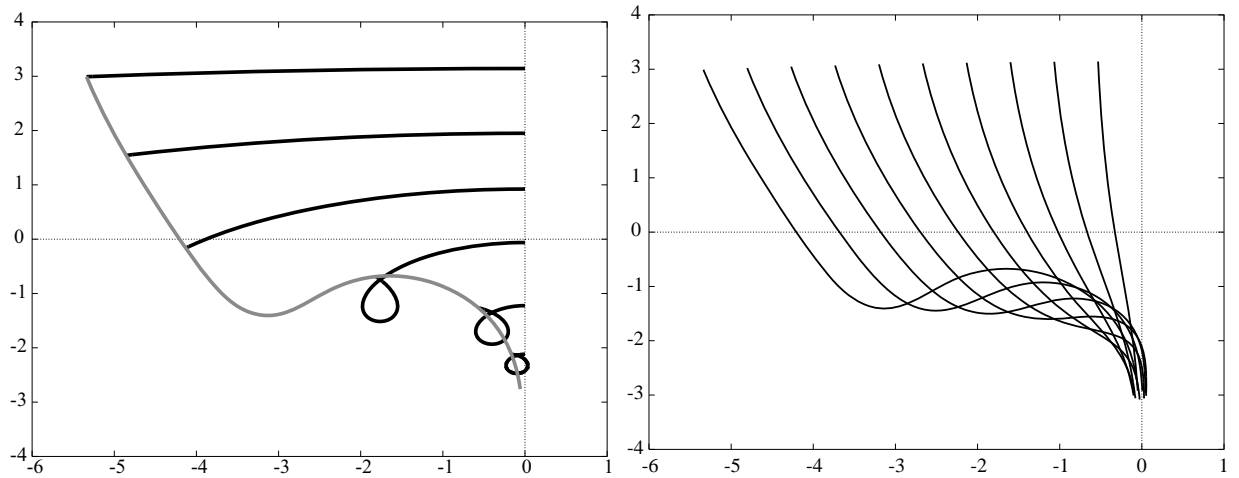

Figure 8: The same as in Figure 7, but $A = 0.44$.

9

For some solutions, $N = 128$ is enough, but some gravity waves requires a large N such as $N = 1024$, see [22]. With these coefficients a_n in hand, we compute

$$\omega(\rho, \sigma) = \theta(\rho, \sigma) + \mathrm{i}\tau(\rho, \sigma) = \sum_{n=1}^{N} a_n \rho^n \sin n\sigma - \mathrm{i} \sum_{n=1}^{N} a_n \rho^n \cos n\sigma = \sum_{n=1}^{N} (-\mathrm{i}) a_n \left(\rho e^{\mathrm{i}\sigma}\right)^n$$

$$= -\mathrm{i} \sum_{n=1}^{N} a_n \zeta^n.$$

and

$$\frac{\mathrm{d}f}{\mathrm{d}z} = \exp\left(-\mathrm{i}\omega\right) = \exp\left(-\sum_{n=1}^{N} a_n \zeta^n\right).$$

As in the case of Crapper's wave, we have

$$\frac{\mathrm{d}\zeta}{\mathrm{d}z} = -\mathrm{i}\zeta \exp\left(-\sum_{n=1}^{N} a_n \zeta^n\right) \qquad \text{or} \qquad \frac{\mathrm{d}z}{\mathrm{d}\zeta} = \frac{\mathrm{i}}{\zeta} \exp\left(\sum_{n=1}^{N} a_n \zeta^n\right). \qquad (19)$$

The velocity is represented as

$$\exp\left(-\sum_{n=1}^{N} a_n \overline{\zeta}^n\right) = \frac{\mathrm{d}z}{\mathrm{d}t} = \frac{\mathrm{i}}{\zeta} \exp\left(\sum_{n=1}^{N} a_n \zeta^n\right) \frac{\mathrm{d}\zeta}{\mathrm{d}t}.$$

Consequently,

$$\frac{\mathrm{d}\zeta}{\mathrm{d}t} = -\mathrm{i}\zeta \exp\left(-\sum_{n=1}^{N} a_n \left(\overline{\zeta}^n + \zeta^n\right)\right) = -\mathrm{i}\zeta \exp\left(-2\sum_{n=1}^{N} a_n \rho^n \cos n\sigma\right)$$

$$= -\mathrm{i}\zeta \exp\left(-\mathrm{i}(\omega - \overline{\omega})\right).$$

This gives us

$$\frac{\mathrm{d}\rho}{\mathrm{d}t} \equiv 0, \qquad \frac{\mathrm{d}\sigma}{\mathrm{d}t} = -\exp\left(-\sum_{n=1}^{N} 2a_n \rho^n \cos n\sigma\right).$$

Therefore ρ is constant along an individual trajectory of a fluid particle. Further,

$$-t = \int_{0}^{\sigma} \exp\left(\sum_{n=1}^{N} 2a_n \rho^n \cos ns\right) \mathrm{d}s \qquad (-\pi \le \sigma \le \pi). \qquad (20)$$

Instead of σ we may use $\sigma' = \pi - \sigma$ and (19) to obtain

$$\frac{\mathrm{d}}{\mathrm{d}\sigma'}(x + \mathrm{i}y) = \exp\left(\sum_{n=1}^{N} a_n(-\rho)^n \cos n\sigma' - \mathrm{i} \sum_{n=1}^{N} a_n(-\rho)^n \sin n\sigma'\right) = \exp(\mathrm{i}\omega(\rho, \pi - \sigma')) \quad (21)$$

$$\frac{\mathrm{d}t}{\mathrm{d}\sigma'} = \exp\left(2\sum_{n=1}^{N} a_n(-\rho)^n \cos n\sigma'\right) = \exp\left(\mathrm{i}\omega - \mathrm{i}\overline{\omega}\right). \qquad (22)$$

10

If the amplitude of the wave is not very large, we may integrate (22) by a simple quadrature rule. Once we have x, y, t as a function of σ', then we can draw

$$X + \mathrm{i}Y = -t + x + \mathrm{i}y.$$

For a fixed ρ, we compute $Y(\rho, 0)$ by

$$Y(\rho, 0) = -\int_\rho^1 \frac{1}{s} \exp\left(\sum_{n=1}^{N} a_n(-s)^n\right) \, \mathrm{d}s.$$

With these formulas we can easily compute trajectories. Figures 9–13 are examples. Longuett-Higgins [20] computes some gravity waves, but it seems to us that trajectories of capillary-gravity waves have not been computed before.
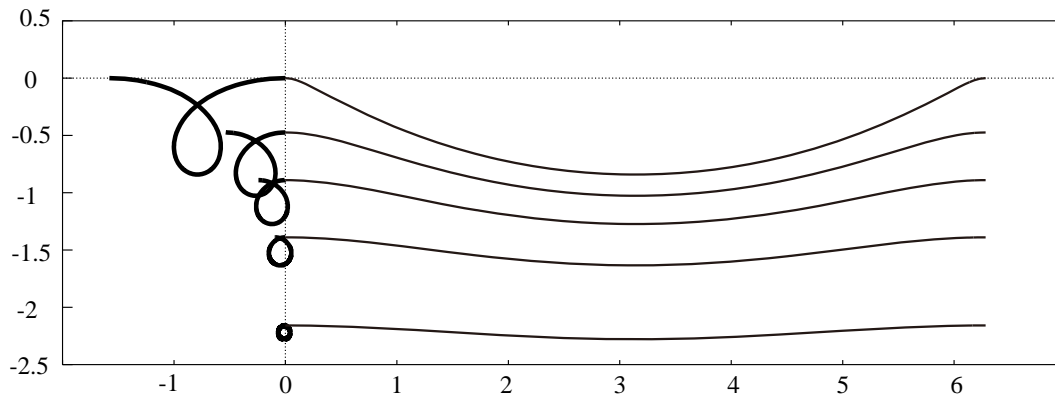

Figure 9: Particle trajectories on and in a gravity wave. $(p, q) = (0.842, 0)$. $\rho = 0.2 \times k$ $(k = 1, 2, \cdots, 5)$.

Figure 9 shows trajectories of fluid particles when $(p, q) = (0.842, 0)$. Numerical data in (18) is borrowed from [22]. Trajectories of five particles $\rho = 0.2 \times k$ $(k = 1, 2, \cdots, 5)$ are plotted. Those on the left hand side are trajectories in stationary coordinates. They start from the y-axis and move leftward. Those on the right hand side (thinner ones) are trajectories in moving coordinates. They start from the y-axis and move rightward until they come to $x = 2\pi$. Figure 10 is a blow-up of the trajectory of $\rho = 0.2$.

In the same fashion, we drew Figures 11–13, where solutions with different (p, q) are chosen, but we took the same ρ, i.e., $\rho = 0.2, \cdots, 1$.

6   Trajectory is not closed.

This section is devoted to a mathematical proof of Constantin's theorem that a particle trajectory is not closed.

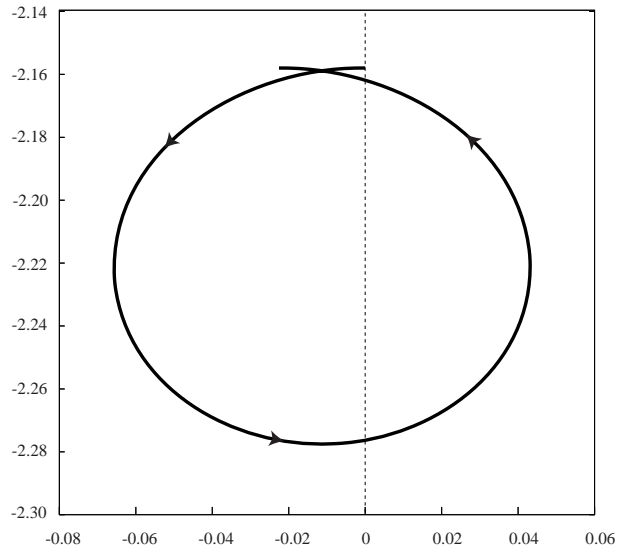## 6.1   The case of infinite depth

We prove

Figure 10: A particle trajectory deep in a gravity wave. $(p, q) = (0.842, 0)$. $\rho = 0.2$.
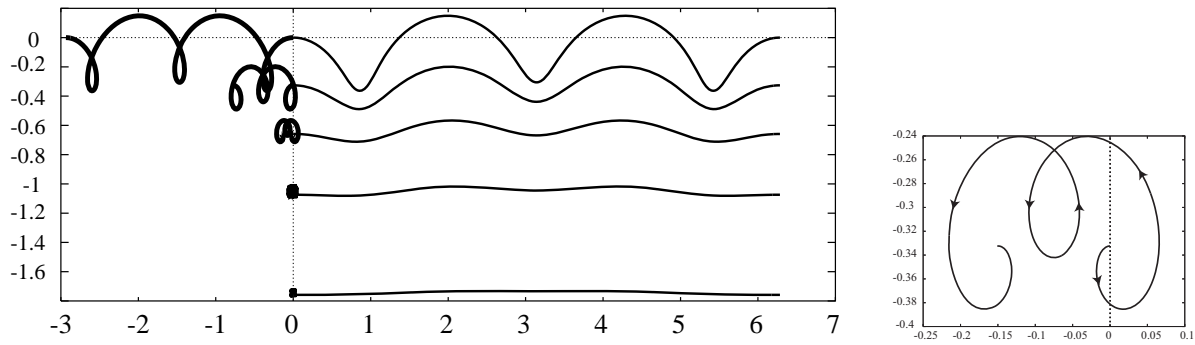

Figure 11: Particle trajectories on and in a capillary-gravity wave. $(p, q) = (0.73, 0.28)$. The trajectory of $\rho = 0.6$ is plotted on the right.
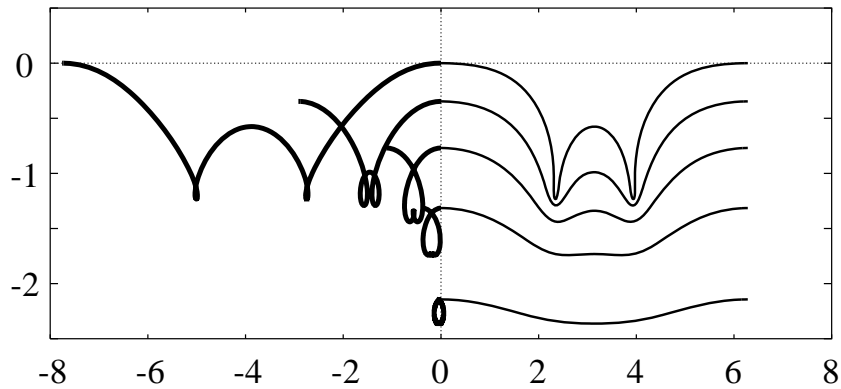

Figure 12: Particle trajectories on and in a capillary-gravity wave. $(p, q) = (0.79, 0.5)$.
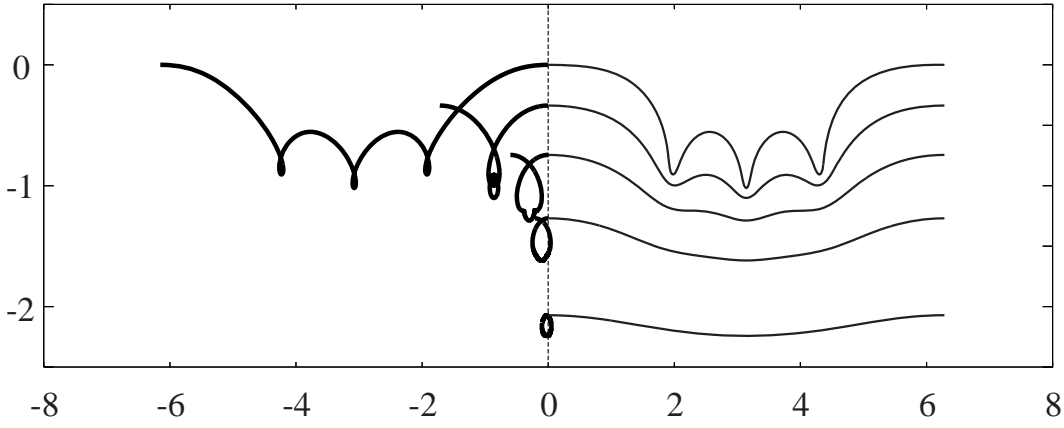
Figure 13: Particle trajectories on and in a capillary-gravity wave. $(p, q) = (0.76, 0.31)$.

Theorem 1 *Suppose that the depth is infinite. Then for any p and q, we have $X\big|_{\sigma'=2\pi} < X\big|_{\sigma'=0}$. Also, $X\big|_{\sigma'=0} - X\big|_{\sigma'=2\pi}$ is monotonically increasing in ρ.*

Proof. What we have to prove is

$$X\big|_{\sigma=\pi} - X\big|_{\sigma=-\pi} > 0.$$

Note first that (21) implies that

$$-x\big|_{\sigma=\pi} + x\big|_{\sigma=-\pi} = \int_{-\pi}^{\pi} \mathrm{Re}\left[\exp(\mathrm{i}\,\omega(\rho, \sigma))\right] \mathrm{d}\sigma.$$

(20) implies that

$$-t\big|_{\sigma=\pi} + t\big|_{\sigma=-\pi} = \int_{-\pi}^{\pi} \left|\exp(\mathrm{i}\,\omega(\rho, \sigma))\right|^2 \mathrm{d}\sigma.$$

Since $X = x - t$, our goal is to prove

$$\int_{-\pi}^{\pi} \mathrm{Re}\left[\exp(\mathrm{i}\,\omega(\rho, \sigma))\right] \mathrm{d}\sigma < \int_{-\pi}^{\pi} \left|\exp(\mathrm{i}\,\omega(\rho, \sigma))\right|^2 \mathrm{d}\sigma. \tag{23}$$

The left hand side is computed as follows:

$$\int_{-\pi}^{\pi} \mathrm{Re}\left[\exp(\mathrm{i}\,\omega(\rho, \sigma))\right] \mathrm{d}\sigma = \mathrm{Re}\left[\int_{-\pi}^{\pi} \exp(\mathrm{i}\,\omega(\rho, \sigma))\, \mathrm{d}\sigma\right] = \mathrm{Re}\left[\int_{|\zeta|=\rho} \exp(\mathrm{i}\,\omega(\zeta)) \frac{\mathrm{d}\zeta}{\mathrm{i}\,\zeta}\right] = 2\pi.$$

The rightmost equality follows from Cauchy's integral formula and $\omega(0) = 0$. (Note that $\omega(0) = 0$ is a consequence of the fact that $\frac{\mathrm{d}f}{\mathrm{d}z} \to 1$ as $y \to -\infty$. See (2).)

Next, we expand the analytic function $\exp(\mathrm{i}\omega(\rho, \sigma))$ into the Taylor expansion:

$$\exp(\mathrm{i}\omega(\rho, \sigma)) = 1 + a_1\zeta + a_2\zeta^2 + \cdots.$$

Then,

$$\int_{-\pi}^{\pi} \left|\exp(\mathrm{i}\omega(\rho, \sigma))\right|^2 \mathrm{d}\sigma = 2\pi\left(1 + |a_1|^2\rho^2 + |a_2|^2\rho^4 + \cdots\right).$$

13

Accordingly, unless $a_1 = a_2 = \cdots = 0$, the inequality (23) holds true. Monotonicity in ρ is obvious.

$\blacksquare$

Corollary 1 *The absolute value of the drift distance is positive, and is the largest on the free surface ($\rho = 1$).*

6.2   The case of finite depth

If we wish to prove that $X\big|_{\sigma=\pi} - X\big|_{\sigma=-\pi} > 0$, in the case of finite depth, we need some modification on the proof above. Let us recall some formulas in [22]. If the depth is specified, we are given a parameter $\eta \in (0, 1)$ and a function $\omega = \theta + i\tau$ which is defined in the annulus $\eta \le |\zeta| \le 1$ and is analytic in $\eta < |\zeta| < 1$. They satisfy the equation (3) on the outer boundary $\rho = 1$, and θ vanishes on the inner boundary $\rho = \eta$. Note that we do not lose generality (see [22]) if we assume that

$$\int_{-\pi}^{\pi} \tau(\rho, \sigma)\, \mathrm{d}\sigma = 0.$$

With this formulas, we have to prove (23), which we can write as

$$\int_{-\pi}^{\pi} e^{-\tau} \cos\theta\, \mathrm{d}\sigma < \int_{-\pi}^{\pi} e^{-2\tau}\, \mathrm{d}\sigma. \tag{24}$$

Theorem 2 *Unless $\theta \equiv 0$, (24) holds true.*

To prove (24) we first note that

$$\int_{-\pi}^{\pi} e^{-\tau} \cos\theta\, \mathrm{d}\sigma < \int_{-\pi}^{\pi} e^{-\tau}\, \mathrm{d}\sigma$$

unless $\theta \equiv 0$. Second, the Hölder inequality gives us

$$\left(\int_{-\pi}^{\pi} e^{-\tau}\, \mathrm{d}\sigma\right)^2 \le 2\pi \int_{-\pi}^{\pi} e^{-2\tau}\, \mathrm{d}\sigma.$$

We finally use Jensen's inequality with a convex function $x \mapsto e^x$ to obtain

$$\frac{1}{2\pi} \int_{-\pi}^{\pi} e^{-\tau}\, \mathrm{d}\sigma \ge \exp\left(-\frac{1}{2\pi} \int_{-\pi}^{\pi} \tau\, \mathrm{d}\sigma\right) = 1.$$

Combining these inequalities, we can conclude that (24) is valid unless $\theta \equiv 0$. $\blacksquare$

We here present some remarks and comparisons. We remark first that in the present case of finite depth, our proof says nothing about monotonicity in ρ. We leave this issue to a future work. Constantin [4] proved the non-closedness of a trajectory in the case of gravity waves of finite depth, although his method is valid in the case of infinite depth, too. See also [16]. Their method is different from ours. Ours is valid in the presence of surface tension, too. It seems to us that the proof in [4, 16] requires an assumption that the wave profile has one and only one relative maximum. We do not need to assume this. Since numerical

14

examples of gravity waves which possess more than one relative maxima in its profile are known (see, [22]), our proof may be worth being recorded. (The capillary-gravity waves in section 5 are also such examples.) A theorem in the case of solitary waves are considered in [5].

Water waves with underlying uniform current is considered in [9]. We can also consider them with underlying shear flow (see chapter 7 of [22]). These constitute further problems, but we leave them to the reader.

7   Conclusion

None of the particle trajectories in the stationary coordinates are closed, although they are very close to a closed circular curve if the fluid particle lies deeply. Fluid particles are pushed out by the wave in the same direction as the wave. The drift distance is the largest on the water surface and decreases exponentially and monotonically in the depth.

Since Gerstner's wave has been the unique example of explicitly written trajectories, our explicit formula for particle trajectory of Crapper's waves may be worthy of notice. The present analysis can be viewed as one of the particle dynamics considered in many situations such as [18, 24].

We are naturally led to a question: if we consider a rotational wave, what is a necessary and sufficient condition for a vorticity distribution to produce closed trajectories only? Our method is restricted to irrotational waves, and does not seem to work in the case of rotational waves. For rotational waves, see chapter 7 of [22] and recent papers [2, 6, 10, 13, 17, 29]. Waves on a sloping beach [3], too, may well give us an interesting problem. We would like to pose this problem to the reader.

References

[1] Y.-Y. Chen, H.-C. Hsu, and G.-Y. Chen, Lagrangian experiment and solution for irrotational finite-amplitude progressive gravity waves at uniform depth, *Fluid Dynam. Res.*, **42** (2010), 045511 (34pp).

[2] A. Constantin, On the deep water wave motion, *J. Phys. A*, **34** (2001), 1405–1417

[3] A. Constantin, Edge waves along a sloping beach, *J. Phys. A*, **34** (2001), 9723–9731.

[4] A. Constantin, The trajectories of particles in Stokes waves, *Invent. Math.* **166** (2006), 523–535.

[5] A. Constantin and J. Escher, Particle trajectories in solitary water waves, *Bull. Amer. Math. Soc.*, **44** (2007), 423–431.

[6] A. Constantin and J. Escher, Analyticity of periodic traveling free surface water waves with vorticity, *Ann. Math.*, **173** (2011), 559–568.

[7] A. Constantin, M. Ehrnström, and G. Villari, Particle trajectories in linear deep-water waves, *Nonlinear Anal: Real world Appl.*, **9** (2008), 1336–1344.

[8] A. Constantin and G. Villari, Particle trajectories in linear water waves, *J. Math. Fluid Mech.*, **10** (2008), 1–18.

[9] A. Constantin and W. Strauss, Pressure beneath a Stokes wave, *Comm. Pure Appl. Math.*, **63** (2010), 0533–0557.

[10] A. Constantin and E. Varvaruca, Steady periodic water waves with constant vorticity: regularity and local bifurcation *Arch. Rational Mech. Anal.*, **199** (2011) 33–67

[11] A. D. D. Craik, The origin of water wave theory, *Ann. Review Fluid Mech.* **36** (2004), 1–28.

[12] G. D. Crapper, An exact solution for progressive capillary waves of arbitrary amplitude, *J. Fluid Mech.*, **2** (1957), 532–540.

[13] M. Ehrnström and G. Villari, Linear water waves with vorticity: Rotational features and particle paths, *J. Diff. Eqns.*, **244** (2008) 1888–1909.

[14] F. Gerstner, Theorie der Wellen, *Abhandlungen der königl. bömischen Gesellschaft der Wissenschaften zu Prag*, (1802), also in *Annalen der Physik*, **32** (1809), 412–445.

[15] G. Green, Note on the motion of waves in canals, in *Mathematical Papers, George Green* ed. N.M. Ferrers, Macmillan (1871), 273–280.

[16] D. Henry, The trajectories of particles in deep-water Stokes waves, *Inter. Math. Res. Notices* **2006**, 1–13.

[17] D. Henry, On Gerstner's water wave, *J. Nonlinear Math. Phys.*, **15** (2008), 87–95.

[18] Y. Kimura and S. Koikari, Particle transport by a vortex soliton, *J. Fluid Mech.* **510**, 201–218

[19] H. Lamb, Hydrodynamics, *Cambridge University Press*, (1932).

[20] M. S. Longuett-Higgins, The trajectories of particles in deep, symmetric gravity waves, *J. Fluid Mech.* **94** (1979), 497–517.

[21] L. M. Milne-Thomson, Theoretical Hydrodynamics, Fifth Edition, *Macmillan* (1968).

[22] H. Okamoto and M. Shōji, The Mathematical Theory of Bifurcation of Permanent Progressive Water-Waves, *World Scientific* (2001).

[23] W. J. M. Rankine, On the exact form of waves near the surface of deep water, *Phil. Trans. Royal Soc. Lond.*, **153** (1863), 127–138

[24] M. Shōji, H. Okamoto, and T. Ooura, Particle trajectories around a running cylinder or a sphere, *Fluid Dynam. Res.* , **42** (2010), 025506.

[25] G. G. Stokes, On the waves of oscillatory waves, *Trans. Camb. Phil. Soc.* **VIII** (1847): *Mathematical and Physical Papers* vol. 1, 197–229.

[26] J. F. Toland, Stokes waves, *Topol. Meth. Nonlinear Anal.*, **7** (1996), 1–48.

[27] M. Umeyama, Coupled PIV and PTV measurements of particle velocities and trajectories for surface waves following a steady current, *J. Waterway, Port, Coastal, Ocean Eng.*, **137** (2010), 85–94.

[28] M. Van Dyke, An Album of Fluid Motion, *Parabolic Press* (1982).

[29] E. Wahlen, Steady water waves with a critical layer, *J. Diff. Eqns.* **246** (2009), 2468–2483